

# Exceptional Dynamical Phase Transitions in Periodically Driven Quantum Systems

Ryusuke Hamazaki

*Nonequilibrium Quantum Statistical Mechanics RIKEN Hakubi Research Team,  
RIKEN Cluster for Pioneering Research (CPR), RIKEN iTHEMS, Wako, Saitama 351-0198, Japan*  
(Dated: May 7, 2022)

Quantum phases and their transitions play a pivotal role to characterize macroscopic matter. Recent studies have revealed that critical transitions reminiscent of equilibrium phase transitions can occur even out of equilibrium, as a singularity of dynamical counterpart of free energy. In this paper, we report a novel mechanism of dynamical phase transitions caused by spontaneous hidden antiunitary-symmetry breaking in periodically driven unitary dynamics. We characterize dynamical phases in such systems with nonunitary many-body operator obtained by switching space and time and find that its symmetry constrains the nature of phases and their transitions. In particular, at some parameters of stroboscopic Ising models, dynamical free energy density exhibits a critical transition with novel singularity absent in equilibrium. The criticality and its universal exponent originate from a many-body exceptional point of the nonunitary operator associated with spontaneous antiunitary-symmetry breaking. We also show that the generalized correlation function has the divergent correlation length at transition and exhibits oscillatory long-range order after symmetry breaking. Our results open up a quest for hitherto unknown phases with their hidden connection to nonunitary physics in macroscopic nonequilibrium systems, which can be tested in state-of-the-art quantum simulators.

*Introduction.* Phase transition [1, 2] is one of the most fundamental collective phenomena in macroscopic systems. Recent experiments on artificial quantum many-body systems [3, 4] motivate researchers to understand phases and their transitions in systems out of equilibrium. Various nonequilibrium phases are proposed including e.g., many-body localized phases [5–8], Floquet topological phases [9–11], and discrete time crystals [12–16]. As a phase transition for transient times, dynamical phase transition (DPT) particularly gathers great attention as a nonequilibrium counterpart of equilibrium phase transition in unitary many-body dynamics [17, 18]. Defined as the singularity of the so-called dynamical free energy (especially at critical times), which is calculated from the unitary operator of dynamics, the DPT has been actively studied theoretically [19–25] and experimentally [26, 27].

Another recently growing field of research, whose relation with the DPT is little known, is the spectral singularity of non-Hermitian systems. When non-Hermitian systems have antiunitary symmetry (AUS) [28–30], such as parity-time symmetry [31, 32], they have a parameter point where two or more eigenstates coincide, leading to the lack of diagonalizability of the Hamiltonian. This point is called an exceptional point and induces spectral singularity unique to nonnormal matrices. The spectral transition through an exceptional point, where eigenstates spontaneously break AUS, have been extensively studied in classical and quantum dissipative systems [33–37]. In particular, strongly correlated non-Hermitian quantum systems with many-body exceptional points are of active theoretical interest [38–40].

In this paper, we show that periodically driven (Floquet) unitary quantum many-body systems can exhibit DPT that originates from an exceptional point of a

nonunitary operator, which is obtained from a nontrivial mapping of the dynamical free energy. We first demonstrate that an experimentally realizable stroboscopic Ising chain, where spins are globally rotated after interactions, shows DPTs through changes of rotation angles. Among them, we find that the derivative of dynamical free energy can diverge for some parameter regimes, which indicates a novel singularity absent in equilibrium phase transition. To understand this, we employ “spacetime dual” of the model (see Fig. 1a), which is yet another notion attracting recent surge of interest, and fully characterize the DPT. Spacetime duality is the way to analyze a unitary operator  $U$  for periodically driven dynamics using a nonunitary dual transfer operator  $\tilde{U}$  obtained by switching the role of space and time [41], recently succeeding in solving certain quantum many-body chaotic systems [42–44] (see Fig. 1(a)). Here, we point out for the first time that symmetries hidden in  $\tilde{U}$  fundamentally affect the DPT. Particularly, the above novel singular DPT occurs when the dual operator has a many-body exceptional point under AUS (Fig. 1(b)): thus we call this DPT an “*exceptional DPT*”. The exceptional DPT is a transition between hidden-AUS-unbroken and broken phases: the generalized correlation function has the divergent correlation length at transition and exhibits oscillatory long-range order after symmetry breaking. Furthermore, we show that AUS also protects distinct dynamical phases, which are captured by the universal bound of finite-size correction of the free energy. Our finding demonstrates that nonunitary physics unravels novel type of nonequilibrium phase transitions via spacetime duality.

*Stroboscopic Ising chains and dynamical free energy.* We consider a one-dimensional quantum stroboscopic spin model [13, 41, 42] composed of Ising interaction and

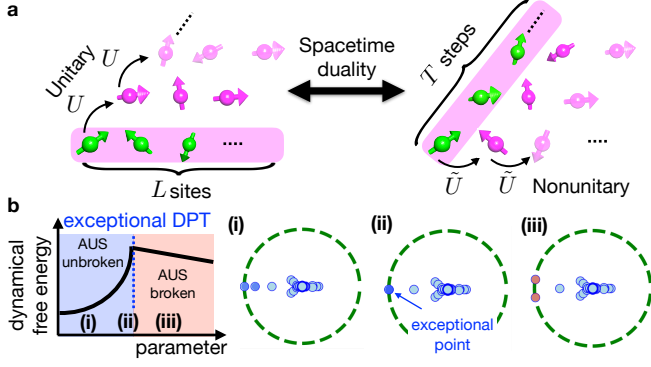


FIG. 1. (a) Schematic of spacetime duality of the Floquet many-body spin systems with size  $L$ . Dynamical free energy densities at step  $T$  calculated from the original unitary evolution  $U$  are equivalent to the trace of  $L$ th power of nonunitary operators  $\tilde{U}$ , which involve complex interaction and rotations of  $T$  spins. (b) For exceptional DPT, free energy has a divergent derivative at some critical parameter. (i)-(iii) The eigenvalues of  $\tilde{U}$  with the green dashed circle indicating the largest modulus (i.e., absolute value) among the eigenvalues, which show the origin of the exceptional DPT. (i) Eigenvalues with the largest and the second largest modulus lie on the same radial direction protected by antiunitary symmetry (AUS) of  $\tilde{U}$  (i.e., AUS is unbroken). (ii) They coincide at the critical parameter and show spectral singularity as an exceptional point. (iii) They then form a complex-conjugate pair (i.e., AUS breaking) and modulus of two eigenvalues becomes equivalent.

subsequent global rotation, which can be realized in experiments of e.g., trapped ions [15]. Its unitary time evolution for a single step can be written as

$$U = e^{-i \sum_{j=1}^L b \sigma_j^x} e^{-i \sum_{j=1}^L J \sigma_j^z \sigma_{j+1}^z} e^{-i \sum_{j=1}^L h \sigma_j^z}, \quad (1)$$

where we impose a periodic boundary condition.

Let us consider a time-evolved state  $U^T |\psi_i\rangle$  after  $T$  steps from an initial state  $|\psi_i\rangle$ . To characterize this nonequilibrium state, we focus on the fidelity with another state  $|\psi_f\rangle$ , i.e.,  $|\langle \psi_f | U^T |\psi_i\rangle|$ . The logarithm of this fidelity per system size,  $F_{L,T}$ , is dubbed as (the real part of) dynamical free energy density [18]. We here mainly consider  $|\psi_i\rangle = |\psi_f\rangle = |\psi\rangle$  and average the fidelity over  $|\psi\rangle$  randomly taken from the unitary Haar measure. Then, the (modified) dynamical free energy density reads

$$F_{L,T}^s(b, J, h) = -\frac{1}{L} \log |\text{Tr}[U^T]| + \log 2. \quad (2)$$

The superscript  $s$  means that  $F_{L,T}^s$  is the logarithm of the spectral form factor [42] up to constant. We also discuss free energy density for other initial and final states, especially  $F_{L,T}^{\uparrow\uparrow}$  corresponding to  $|\psi_i\rangle = |\psi_f\rangle = \bigotimes_{j=1}^L |\uparrow_j\rangle$ , where  $|\uparrow_j\rangle/|\downarrow_j\rangle$  is the eigenstate of  $\sigma_j^z$  with an eigenvalue

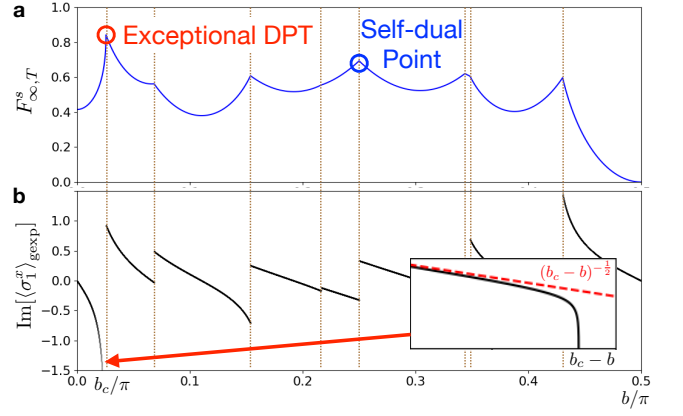


FIG. 2. (a) Dynamical free energy density  $F_{\infty,T}^s$ , whose cusp indicates DPT, as a function of the rotation angle  $b$ . Among DPTs, we have the exceptional DPT (red circle), which shows divergent derivative, and the DPT crossing the self-dual point (blue circle). (b) Imaginary part of the generalized expectation value given in Eq. (3), which is proportional to the  $b$ -derivative of  $F_{\infty,T}^s$ . While it exhibits a jump for typical DPTs, it diverges at the exceptional DPT. (inset) The divergence obeys  $(b_c - b)^{-1/2}$  (red dashed line). We use  $J = -\pi/4$  and  $h = 3.0$ , and  $T = 6$ .

$+1/-1$ , and  $F_{L,T}^{\downarrow\uparrow}$  corresponding to  $|\psi_i\rangle = \bigotimes_{j=1}^L |\uparrow_j\rangle$  and  $|\psi_f\rangle = \bigotimes_{j=1}^L |\downarrow_j\rangle$ .

The derivative of  $F_{L,T}$  gives the (imaginary part of) so-called generalized expectation values. For example, we have

$$-\frac{1}{T} \frac{dF_{L,T}^s}{db} = \text{Im} \left[ \text{Tr} \left( \frac{1}{L} \sum_j \sigma_j^x \tilde{\rho} \right) \right] := \text{Im} [\langle \sigma_1^x \rangle_{\text{geexp}}], \quad (3)$$

where  $\tilde{\rho} = U^T / \text{Tr}[U^T]$  and we have used translation invariance. Importantly, the dynamical free energy density and the generalized expectation values can be in principle measured with an interferometric experiment [18, 22].

We seek for singularity of  $F_{\infty,T}$  when some continuous parameter is varied. In Ref. [17],  $F_{\infty,T}$  exhibits singularity at critical times for continuous-time models. Since  $T$  is discrete in our model, instead of changing  $T$ , we consider continuously changing other parameters (such as  $b$ ) for fixed  $T$ .

*Dynamical phases and their transitions.* As a prime example that highlights our discovery, we show in Fig. 2 the (real-part of) dynamical free energy density  $F_{\infty,T(=6)}^s$  and  $\text{Im}[(\sigma_1^x)_{\text{geexp}}]$  as a function of rotation angle  $b$  for  $J = -\pi/4$  and  $h = 3.0$  (see Supplemental Material for the data with other parameters and initial/final states [45]). This is calculated from the eigenvalue with the largest modulus of the space-time dual operator, as detailed later. We find different singular behaviors for  $F_{\infty,T}^s$ , sig-

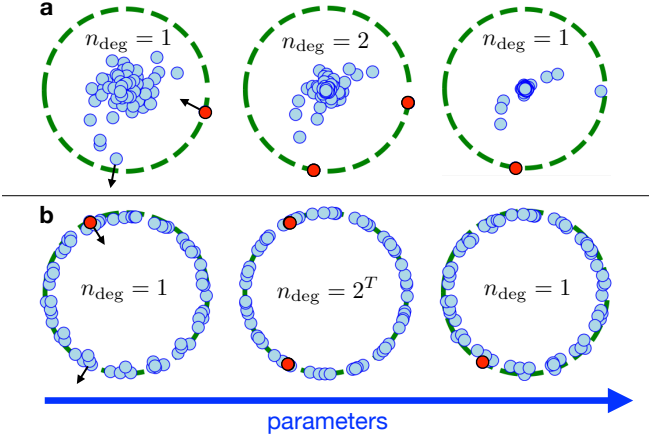


FIG. 3. (a) Schematic of typical eigenvalue dynamics of  $\tilde{U}$  (small circles) near DPT. Green dashed circles have the radius that corresponds to the eigenvalue(s) with the largest modulus. The eigenvalue with the largest modulus (red circles) switches at the critical point, at which two eigenvalues have the same modulus  $n_{\text{deg}} = 2$ . (b) Eigenvalue dynamics through the DPT induced by self-dual points. At the self-dual point, all of  $2^T$  numbers of eigenvalues have the same modulus owing to the unitarity of  $\tilde{U}$ .

nalizing distinct dynamical phase transitions at critical parameters. First, we find many cusps of  $F_{\infty,T}^s$  with varying  $b$ , across which  $\text{Im}[\langle \sigma_1^x \rangle_{\text{gexp}}]$  exhibits a finite jump. While they are analogous to (continuous time) DPTs studied previously, we here stress the importance of transition points at  $J = \frac{\pi}{4} + \frac{n\pi}{2}$  and  $b = \frac{\pi}{4} + \frac{m\pi}{2}$  ( $n, m \in \mathbb{Z}$ ), which are known as self-dual points in the context of quantum many-body chaos [42, 43]. As discussed later, crossing self-dual points entails DPT universally for  $F_{\infty,T}^{s/\uparrow\downarrow}$  with any  $T$  and  $h$ . There, the dynamical free energy density takes a universal value as  $F_{\infty,T}^s = \log 2$  or  $F_{\infty,T}^{\uparrow\downarrow} = \log 2/2$ .

Notably, we find a novel singularity at  $b = b_c \simeq 0.0257$ , where the derivative diverges as  $\frac{dF_{\infty,T}^s}{db} \propto \text{Im}[\langle \sigma_1^x \rangle_{\text{gexp}}] \sim |b_c - b|^{-1/2}$  for  $b \lesssim b_c$ . Such a strong singularity is prohibited for equilibrium free energy density, since thermal expectation value of a local observable cannot diverge. We call this transition an *exceptional DPT*, since it originates from the occurrence of an exceptional point of a nonunitary operator that is dual to  $U$ . As shown below, an exceptional DPT can occur only for  $F_{\infty,T}^{s/\uparrow\downarrow}$  with  $J = \frac{\pi}{4} + \frac{n\pi}{2}$  ( $n \in \mathbb{Z}$ ) and even/odd  $T$  and is robust under certain weak perturbation (such as  $h$ ), which is deeply related to the hidden symmetry of our setup.

*Spacetime duality and hidden symmetries.* To understand the above behaviors, we employ the space-time duality [41] of our Floquet operator. This is an exact method to switch the role of time and space, and rewrite  $U^T$  with  $L$  product of a space-time-dual transfer ma-

trix  $\tilde{U}$ , which involves  $T$  spins. We can exactly write  $F_{L,T} = -\log |\text{Tr}[\tilde{U}^L]|/L$ , where, for example,

$$\tilde{U}_s = C e^{-i \sum_{\tau=1}^T \tilde{b} \sigma_{\tau}^x} e^{-i \sum_{\tau=1}^T \tilde{J} \sigma_{\tau}^z \sigma_{\tau+1}^z} e^{-i \sum_{\tau=1}^T h \sigma_{\tau}^z} \quad (4)$$

with the periodic boundary condition for  $F_{L,T}^s$  [41–43] (see Supplemental Material [45] for the proof and the discussion for  $\tilde{U}^{\uparrow\uparrow/\downarrow\downarrow}$ , which corresponds to  $F_{L,T}^{\uparrow\uparrow/\downarrow\downarrow}$ ). Here,  $\tilde{b} = -\pi/4 - i \log(\tan J)/2$ ,  $\tilde{J} = -\pi/4 - i \log(\tan b)/2$  and  $C = (\sin 2b / \sin 2\tilde{b})^{T/2}/2$ . Importantly,  $\tilde{U}$  is unitary (up to a constant) only at the self-dual points.

Let  $\lambda_{M,\alpha} = |\lambda_M| e^{i\theta_{\alpha}}$  be eigenvalues of  $\tilde{U}$  whose modulus gives the largest one among all eigenvalues. Here,  $\alpha = (1, \dots, n_{\text{deg}})$  is the label of the degeneracy, where  $n_{\text{deg}}$  is the number of eigenvalues giving the maximum modulus. For large  $L$ ,  $F_{L,T}$  is dominated by these largest eigenvalues, i.e.,

$$F_{L,T} \simeq -\log |\lambda_M| - \frac{1}{L} \log \left| \sum_{\alpha} e^{i\theta_{\alpha} L} \right|. \quad (5)$$

In the thermodynamic limit, the second term vanishes.

As noted previously [21], DPT occurs when the eigenstate that gives the largest eigenvalue switches. For typical cases, DPT occurs when maximum of two eigenvalues with different  $\theta_{\alpha}$  switches accidentally, where  $n_{\text{deg}} = 1$  for each phase and  $n_{\text{deg}} = 2$  at transition (Fig. 3(a)). On the other hand, DPT occurs more universally if the self-dual point is crossed: all of the modulus of the eigenvalues of  $\tilde{U}$  are equal at this point ( $n_{\text{deg}} = 2^T$ ), and crossing this point typically switches the largest eigenvalue (Fig. 3(b)). At transition, dynamical free energies are determined only by the modulus of the eigenvalues, which lead to universal values  $F_{\infty,T}^s = \log 2$  and  $F_{\infty,T}^{\uparrow\downarrow} = \log 2/2$ . To our best knowledge, this is the first evidence that self-dual point is a critical point of different dynamical phases.

Moreover, novel dynamical phases and transitions can appear when  $\tilde{U}$  possesses AUS, i.e.,  $V \tilde{U}^* V^{\dagger} = e^{i\phi} \tilde{U}$  for some unitary operator  $V$  and  $\phi \in \mathbb{R}$ . According to recent classification of non-Hermitian systems [30],  $\tilde{U}$  is called Class A without AUS, Class AI when  $V$  with  $V V^* = \mathbb{I}$  exists, and Class AII when  $V$  with  $V V^* = -\mathbb{I}$  exists. If we consider  $\phi = 0$  without loss of generality, the eigenvalues of  $\tilde{U}$  in Class AI are either real or form complex conjugate pairs. Furthermore, at certain parameters, two real eigenvalues collide and form a complex conjugate pair, which can be called spontaneous AUS-breaking transition. In fact, while eigenstates  $|\phi\rangle$  are symmetric under AUS in the AUS-unbroken phase, i.e.,  $V|\phi\rangle^* = |\phi\rangle$ ,  $V|\phi\rangle^*$  and  $|\phi\rangle$  are different in the AUS-broken phase. At the transition point, known as the exceptional point, two eigenstates become equivalent, which offers a unique feature for nonnormal matrices. In Class AII, on the other hand, eigenvalues generically form complex conju-

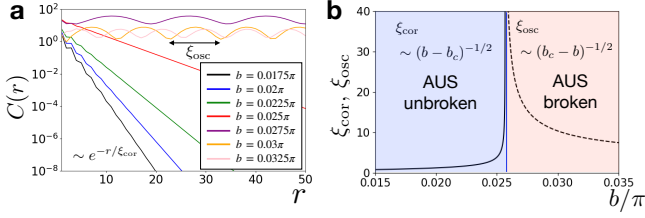


FIG. 4. **Generalized correlation function and correlation/oscillation lengths  $\xi_{\text{cor}}, \xi_{\text{osc}}$ .** (a) Generalized correlation function  $C(r)$  for different values of  $b$  for  $L = 500$ . In the AUS-unbroken phase ( $b < b_c \simeq 0.0257\pi$ ), the correlation decays exponentially. In the AUS-broken phase ( $b > b_c$ ), the correlation exhibits oscillatory long-range order. (b) Divergence of  $\xi_{\text{cor}}$  (solid line) and  $\xi_{\text{osc}}$  (dotted line) in the thermodynamic limit. Approaching the exceptional DPT, they both behave as  $\sim |b - b_c|^{-1/2}$ . We use  $J = -\pi/4$  and  $h = 3.0$ , and  $T = 6$ .

gate pairs and are not real in the presence of the level repulsion [46].

Our Floquet operators  $U$  have such hidden antiunitary symmetries of  $\tilde{U}$  for  $J = \frac{\pi}{4} + \frac{n\pi}{2}$  ( $n \in \mathbb{Z}$ ): indeed, we find  $V = \prod_{\tau=1}^T e^{i\frac{\pi}{2}\sigma_\tau^y}$  for  $\tilde{U}_s$  and  $V = \mathcal{P} \prod_{\tau=1}^{T-1} e^{i\frac{\pi}{2}\sigma_\tau^y}$  for  $\tilde{U}_{\downarrow\uparrow}$ , where  $\mathcal{P}$  is the parity operator exchanging  $\tau$  and  $T - \tau$  [45]. Since  $VV^*$  takes either  $+1$  or  $-1$  depending on  $T$ , we find that  $\tilde{U}_s$  belongs to Class AI for even  $T$  and AII for odd  $T$ , and that  $\tilde{U}_{\downarrow\uparrow}$  belongs to Class AI for odd  $T$  and AII for even  $T$  as long as  $J = \frac{\pi}{4} + \frac{n\pi}{2}$  ( $n \in \mathbb{Z}$ ). In contrast,  $\tilde{U}_{\uparrow\uparrow}$  does not have AUS and belongs to Class A in general.

The above symmetries clearly explain the origin of the exceptional DPT: as shown in Fig. 1(b), this transition occurs when eigenvalues with the largest and the second modulus collide under Class AI AUS, i.e., at the many-body exceptional point for  $\lambda_M$ . It is known that this (second-order) exceptional point entails a universal spectral singularity, where the gap between two eigenvalues behave like  $|b - b_c|^{1/2}$ . This leads to the previously-mentioned notable divergence of the generalized expectation value  $\sim (b_c - b)^{-1/2}$  for  $b < b_c$ , where  $-1/2$  is also known to be a universal critical exponent.

The phases with  $b < b_c$  and  $b > b_c$  correspond to hidden AUS-unbroken and AUS-broken phases, respectively. This is highlighted by the generalized correlation function,  $C(r) = |\langle \sigma_1^z \sigma_{r+1}^z \rangle_{\text{gexp}} - \langle \sigma_1^z \rangle_{\text{gexp}} \langle \sigma_{r+1}^z \rangle_{\text{gexp}}|$  (see Fig. 4 and Supplemental Material [45]). While  $C(r)$  decays exponentially as  $\sim e^{-r/\xi_{\text{cor}}}$  in the AUS-unbroken phase, the correlation length diverges as  $\xi_{\text{cor}} \sim (b_c - b)^{-1/2}$  as it approaches the exceptional DPT point. At AUS-broken phases,  $\xi_{\text{cor}}$  diverges and long-range order appears. Notably, we find that  $C(r)$  oscillates with the oscillation length  $\xi_{\text{osc}}$ , which also diverges near the exceptional DPT  $\xi_{\text{osc}} \sim (b - b_c)^{-1/2}$ . We remark that qualitative signature of the transition can be captured by

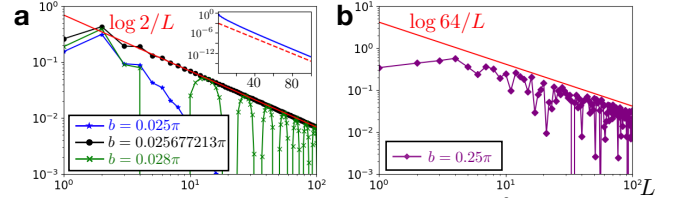


FIG. 5. **Log-log plot for finite-size correction of the dynamical free energy density  $\Delta F_{L,T}^s$ .** (a) Behavior near the exceptional DPT. Below the DPT with  $n_{\text{deg}} = 1$  (blue),  $\Delta F_{L,T}^s$  decays rapidly. (inset) Semi-log plot of the same data shows that it indeed decays exponentially (dotted red line is an eyeguide for exponential decay). Above the DPT with  $n_{\text{deg}} = 2$  (green),  $\Delta F_{L,T}^s$  decays with oscillations. The decay is bounded by  $\log 2/L$  (red solid line) for sufficiently large  $L$ . Approaching the critical point (black), the oscillation vanishes and  $\Delta F_{L,T}^s \sim \log 2/L$ . (b) Behavior at the self-dual point (purple), where  $n_{\text{deg}} = 2^T = 64$ . The correction is bounded by  $\log 64/L$ . We use  $J = -\pi/4$  and  $h = 3.0$ , and  $T = 6$ .

the existence of the long-range order even for relatively small systems [45], which are relevant for experiments.

The discussion on hidden Class AI AUS also enables us to identify the necessary condition for having exceptional DPT. In our prototypical stroboscopic Ising model, we can observe the exceptional DPT by considering  $F_{L,T}^s$  with even  $T$  and  $F_{L,T}^{\downarrow\uparrow}$  with odd  $T$  under the condition  $J = \pi/4$ . Indeed,  $F_{L,T}^{\downarrow\uparrow}$  with  $T = 7$  shows the exceptional DPT for  $b \simeq 0.457\pi$  and  $h = 2$  [45]. Note that this transition is robust even if the value of  $h$  is slightly perturbed, since the transition is protected by AUS.

*Degeneracy and finite-size effect.* While the number of eigenvalues with maximum modulus  $n_{\text{deg}}$  does not contribute to the free energy density for  $L \rightarrow \infty$ ,  $n_{\text{deg}}$  can characterize each phase via a finite-size correction  $\Delta F_{L,T} = F_{L,T} - F_{\infty,T}$ . Indeed, the second term in Eq. (5) shows that  $\Delta F_{L,T}$  is upper bounded by  $\log n_{\text{deg}}/L$ , where the bound is achieved when  $e^{i\theta_\alpha L} = e^{i\theta_\beta L}$  for every  $\alpha \neq \beta$ .

Figure 5(a) shows the finite-size scaling of  $\Delta F_{L,T}$  near the exceptional DPT. While  $\Delta F_{L,T}$  exponentially decays with  $L$  for  $b < b_c$  since  $n_{\text{deg}} = 1$ , it exhibits polynomially decaying oscillations for  $b > b_c$ , where the decay is upper bounded by  $\log n_{\text{deg}}/L = \log 2/L$  for sufficiently large  $L$ . At the transition point, oscillation-free polynomial decay is observed. Another example is the behavior at the self-dual point, where the decay is upper bounded by  $\log 2^T/L$  (Fig. 5(b)).

The number  $n_{\text{deg}}$  thus provides universal information through  $\Delta F_{L,T}$  on dynamical phases, which is deeply related to the symmetries hidden in the space-time dual operator  $\tilde{U}$ . If  $\tilde{U}$  is in Class AI ( $F_{L,T}^s$  with even  $T$  and  $F_{L,T}^{\downarrow\uparrow}$  with odd  $T$  under the condition  $J = \pi/4$ ), phases with  $n_{\text{deg}} = 2$  can naturally appear as well as phases

with  $n_{\text{deg}} = 1$ . If  $\tilde{U}$  is in Class AII ( $F_{L,T}^s$  with odd  $T$  and  $F_{L,T}^{\downarrow\uparrow}$  with even  $T$  under the condition  $J = \pi/4$ ), all phases satisfy  $n_{\text{deg}} \geq 2$ . We note that other symmetries are found to exist that enhance the value of  $n_{\text{deg}}$ , such as translation invariance for  $\tilde{U}_s$  or integrability at  $h = 0$ , which may also be interesting to study systematically.

*Discussions.* Phase transitions were investigated in terms of non-Hermitian operators since the seminal work by Lee, Yang [47, 48] and Fisher [49]. Particularly, phase transitions occur when the zeros of the partition function  $e^{-LF_{L,T}}$ , whose parameter (especially  $b$  in our context) regime is extended to a complex one, accumulate at real values in the thermodynamic limit [18, 49]. Accumulation points of the partition-function zeros are thus read out from the points where maximum eigenvalues switch when we add proper perturbation  $\delta b (\in \mathbb{C})$  whose magnitude is infinitesimal [21]. Notably, the partition-function zeros accumulate along the real axis when the complex-conjugate pair contributes to maximum eigenvalues with  $n_{\text{eff}} = 2$  owing to AUS of  $\tilde{U}$ . This is because one of the eigenvalues that form the complex conjugate at  $b \in \mathbb{R}$  becomes larger and smaller than the other for  $b + \delta b$  and  $b - \delta b$  ( $\delta b \in i\mathbb{R}$ ), respectively. Moreover, we find that these zeros on the real axis (say  $b \geq b_c$ ) terminate at exceptional DPT ( $b = b_c$ ). This means that the exceptional DPT corresponds to the realization of the edge singularity of the partition-function zeros at physical parameters on the real axis, in contrast with previous works [47–49].

We next discuss generalization of our results. We can change other parameters like  $h$  and  $J$  instead of  $b$ . Since AUS of  $\tilde{U}^{s/\downarrow\uparrow}$  is preserved for  $J = \pi/4$ , changing  $h$  can also lead to exceptional DPT for even/odd  $T$ , meaning that  $\langle \sigma_i^z \rangle_{\text{gexp}}$  diverges. On the other hand, changing  $J$  does not lead to exceptional DPT: crossing  $J = \frac{\pi}{4} + \frac{n\pi}{2}$  ( $n \in \mathbb{Z}$ ) instead can lead to the normal DPT when  $n_{\text{deg}}$  is two at the crossing point owing to AUS. This is always the case for  $\tilde{U}^{s/\downarrow\uparrow}$  with odd  $T$ . We also stress that the exceptional DPT is not restricted to the stroboscopic Ising model but occurs for a broader class of Floquet systems, as shown in Supplemental Material [45].

To conclude, we find a new type of universal dynamical phase transition in Floquet quantum many-body systems. Particularly, we show that strong singularity appears at the antiunitary-symmetry breaking across the exceptional point, which are hidden in the spacetime dual nonunitary operator of the original unitary dynamics. Our method via spacetime duality paves the way to study completely new type of phase transitions for quantum many-body unitary dynamics through the scope of nonunitary many-body physics. One of the promising directions is to classify such dynamical phases by the symmetries of the spacetime-dual operator, which are completely classified only recently [28, 30].

We thank Kohei Kawabata for helpful comments on antiunitary symmetry, and Keiji Saito and Mamiko Tat-

suta for fruitful comments on the manuscript. The numerical calculations were carried out with the help of QUSPIN [50].

- 
- [1] L. D. Landau and E. M. Lifshitz, *Statistical Physics: Volume 5*, Vol. 5 (Elsevier, 2013).
  - [2] S. Sachdev, *Handbook of Magnetism and Advanced Magnetic Materials* (2007).
  - [3] H. Bernien, S. Schwartz, A. Keesling, H. Levine, A. Omran, H. Pichler, S. Choi, A. S. Zibrov, M. Endres, M. Greiner, *et al.*, *Nature* **551**, 579 (2017).
  - [4] J. Zhang, G. Pagano, P. W. Hess, A. Kyprianidis, P. Becker, H. Kaplan, A. V. Gorshkov, Z.-X. Gong, and C. Monroe, *Nature* **551**, 601 (2017).
  - [5] A. Pal and D. A. Huse, *Phys. Rev. B* **82**, 174411 (2010).
  - [6] M. Schreiber, S. S. Hodgman, P. Bordia, H. P. Lüschen, M. H. Fischer, R. Vosk, E. Altman, U. Schneider, and I. Bloch, *Science* **349**, 842 (2015).
  - [7] J.-y. Choi, S. Hild, J. Zeiher, P. Schauf, A. Rubio-Abadal, T. Yefsah, V. Khemani, D. A. Huse, I. Bloch, and C. Gross, *Science* **352**, 1547 (2016).
  - [8] J. Smith, A. Lee, P. Richerme, B. Neyenhuis, P. W. Hess, P. Hauke, M. Heyl, D. A. Huse, and C. Monroe, *Nature Physics* **12**, 907 (2016).
  - [9] T. Kitagawa, E. Berg, M. Rudner, and E. Demler, *Phys. Rev. B* **82**, 235114 (2010).
  - [10] N. H. Lindner, G. Refael, and V. Galitski, *Nature Physics* **7**, 490 (2011).
  - [11] M. C. Rechtsman, J. M. Zeuner, Y. Plotnik, Y. Lumer, D. Podolsky, F. Dreisow, S. Nolte, M. Segev, and A. Szameit, *Nature* **496**, 196 (2013).
  - [12] D. V. Else, B. Bauer, and C. Nayak, *Phys. Rev. Lett.* **117**, 090402 (2016).
  - [13] N. Y. Yao, A. C. Potter, I.-D. Potirniche, and A. Vishwanath, *Phys. Rev. Lett.* **118**, 030401 (2017).
  - [14] S. Choi, J. Choi, R. Landig, G. Kucsko, H. Zhou, J. Isoya, F. Jelezko, S. Onoda, H. Sumiya, V. Khemani, *et al.*, *Nature* **543**, 221 (2017).
  - [15] J. Zhang, P. Hess, A. Kyprianidis, P. Becker, A. Lee, J. Smith, G. Pagano, I.-D. Potirniche, A. C. Potter, A. Vishwanath, *et al.*, *Nature* **543**, 217 (2017).
  - [16] R. Moessner and S. L. Sondhi, *Nature Physics* **13**, 424 (2017).
  - [17] M. Heyl, A. Polkovnikov, and S. Kehrein, *Phys. Rev. Lett.* **110**, 135704 (2013).
  - [18] M. Heyl, *Reports on Progress in Physics* **81**, 054001 (2018).
  - [19] C. Karrasch and D. Schuricht, *Phys. Rev. B* **87**, 195104 (2013).
  - [20] M. Heyl, *Phys. Rev. Lett.* **113**, 205701 (2014).
  - [21] F. Andraschko and J. Sirker, *Phys. Rev. B* **89**, 125120 (2014).
  - [22] E. Canovi, P. Werner, and M. Eckstein, *Phys. Rev. Lett.* **113**, 265702 (2014).
  - [23] M. Heyl, *Phys. Rev. Lett.* **115**, 140602 (2015).
  - [24] J. C. Budich and M. Heyl, *Phys. Rev. B* **93**, 085416 (2016).
  - [25] B. Žunkovič, M. Heyl, M. Knap, and A. Silva, *Phys. Rev. Lett.* **120**, 130601 (2018).
  - [26] P. Jurcevic, H. Shen, P. Hauke, C. Maier, T. Brydges,

- C. Hempel, B. P. Lanyon, M. Heyl, R. Blatt, and C. F. Roos, *Phys. Rev. Lett.* **119**, 080501 (2017).
- [27] N. Fläschner, D. Vogel, M. Tarnowski, B. Rem, D.-S. Lühmann, M. Heyl, J. Budich, L. Mathey, K. Sengstock, and C. Weitenberg, *Nature Physics* **14**, 265 (2018).
- [28] Z. Gong, Y. Ashida, K. Kawabata, K. Takasan, S. Higashikawa, and M. Ueda, *Phys. Rev. X* **8**, 031079 (2018).
- [29] K. Kawabata, S. Higashikawa, Z. Gong, Y. Ashida, and M. Ueda, *Nature Communications* **10**, 297 (2019).
- [30] K. Kawabata, K. Shiozaki, M. Ueda, and M. Sato, *Phys. Rev. X* **9**, 041015 (2019).
- [31] C. M. Bender and S. Boettcher, *Phys. Rev. Lett.* **80**, 5243 (1998).
- [32] C. M. Bender, D. C. Brody, and H. F. Jones, *Phys. Rev. Lett.* **89**, 270401 (2002).
- [33] A. Guo, G. J. Salamo, D. Duchesne, R. Morandotti, M. Volatier-Ravat, V. Aimez, G. A. Siviloglou, and D. N. Christodoulides, *Phys. Rev. Lett.* **103**, 093902 (2009).
- [34] C. E. Rüter, K. G. Makris, R. El-Ganainy, D. N. Christodoulides, M. Segev, and D. Kip, *Nature Physics* **6**, 192 (2010).
- [35] J. Li, A. K. Harter, J. Liu, L. de Melo, Y. N. Joglekar, and L. Luo, *Nature communications* **10**, 855 (2019).
- [36] R. El-Ganainy, K. G. Makris, M. Khajavikhan, Z. H. Musslimani, S. Rotter, and D. N. Christodoulides, *Nature Physics* **14**, 11 (2018).
- [37] M.-A. Miri and A. Alù, *Science* **363**, eaar7709 (2019).
- [38] Y. Ashida, S. Furukawa, and M. Ueda, *Nature Communications* **8**, 15791 (2017).
- [39] R. Hamazaki, K. Kawabata, and M. Ueda, *Phys. Rev. Lett.* **123**, 090603 (2019).
- [40] D. J. Luitz and F. Piazza, *Phys. Rev. Research* **1**, 033051 (2019).
- [41] M. Akila, D. Waltner, B. Gutkin, and T. Guhr, *Journal of Physics A: Mathematical and Theoretical* **49**, 375101 (2016).
- [42] B. Bertini, P. Kos, and T. Prosen, *Phys. Rev. Lett.* **121**, 264101 (2018).
- [43] B. Bertini, P. Kos, and T. Prosen, *Phys. Rev. X* **9**, 021033 (2019).
- [44] B. Bertini, P. Kos, and T. c. v. Prosen, *Phys. Rev. Lett.* **123**, 210601 (2019).
- [45] See Supplemental Material for the details on dynamical phase transitions for other parameters and initial/final states, derivation of spacetime-dual operators, details on time-reversal symmetry, discussion for generalized correlation function, and other models that exhibit exceptional dynamical phase transition.
- [46] R. Hamazaki, K. Kawabata, N. Kura, and M. Ueda, *Phys. Rev. Research* **2**, 023286 (2020).
- [47] T. D. Lee and C. N. Yang, *Phys. Rev.* **87**, 410 (1952).
- [48] C. N. Yang and T. D. Lee, *Phys. Rev.* **87**, 404 (1952).
- [49] M. E. Fisher, *Phys. Rev. Lett.* **40**, 1610 (1978).
- [50] P. Weinberg and M. Bukov, *SciPost Phys* **7**, 020 (2019).



# Supplemental Material for “Exceptional Dynamical Phase Transitions in Periodically Driven Quantum Systems”

Ryusuke Hamazaki

*Nonequilibrium Quantum Statistical Mechanics RIKEN Hakubi Research Team,  
RIKEN Cluster for Pioneering Research (CPR), RIKEN iTHEMS, Wako, Saitama 351-0198, Japan*

(Dated: May 7, 2022)

## SUPPLEMENTAL NOTE 1: DYNAMICAL PHASE TRANSITIONS FOR OTHER PARAMETERS AND INITIAL/FINAL STATES

Here, we describe in detail dynamical phases and their transitions of the stroboscopic Ising model for situations different from that presented in the main text. Figure S-1 shows examples of dynamical phase transitions (DPT) of  $F_{\infty,T}^s$  for  $T = 7$  and  $T = 8$  with  $J = 0.25\pi$  with varying  $b$ . As discussed in the main text,  $n_{\text{eff}}$  is always larger than 2 or  $T = 7$  because the system belongs to Class AII ( $n_{\text{eff}} \geq 4$  comes from additional symmetry  $\tilde{U}$ , such as the translation invariance). Therefore no exceptional DPT occurs in this case. On the other hand, we find exceptional DPT for  $T = 8$ , indicating that the exceptional DPT is the general mechanism that can occur in systems with Class AI antiunitary symmetry.

Next, Figure S-2(a) shows that the exceptional DPT can occur for  $J = 0.25\pi$  even when  $h$  is varied for fixed appropriate  $b$ , which indicates the divergence of the generalized observable  $\langle \sigma_1^z \rangle_{\text{gexp}}$ . On the other hand, the exceptional DPT does not occur if  $J$  is varied, since antiunitary symmetry no longer exists in  $\tilde{U}$  (Fig. S-2(b)).

Finally, Fig. S-3 shows the  $b$ -dependence of  $F_{\infty,T}^{\uparrow\uparrow}$  and  $F_{\infty,T}^{\downarrow\downarrow}$  for  $J = 0.25\pi$  and  $T = 7$ . As detailed in Supplemental Note 3,  $\tilde{U}_{\downarrow\uparrow}$  has Class AI antiunitary symmetry for odd  $T$ , but  $\tilde{U}_{\uparrow\uparrow}$  does not. Thus, while we can find the exceptional DPT for  $F_{\infty,T}^{\downarrow\downarrow}$  but not for  $F_{\infty,T}^{\uparrow\uparrow}$ .

## SUPPLEMENTAL NOTE 2: DERIVATION OF SPACETIME-DUAL OPERATORS

Here, we describe in detail the derivation of the spacetime-dual operators to calculate the dynamical free energies, following Refs. [1–3]. We first consider the representation for  $\tilde{U}_s$ . For this purpose, we notice

$$\begin{aligned} \text{Tr}[U^T] &= \sum_{\{\mathbf{s}_\tau\}} \prod_{\tau=1}^T \langle \mathbf{s}_{\tau+1} | e^{-i \sum_{j=1}^L b \sigma_j^x} e^{-i \sum_{j=1}^L J \sigma_j^z \sigma_{j+1}^z} e^{-i \sum_{j=1}^L h \sigma_j^z} | \mathbf{s}_\tau \rangle \\ &= \left( \frac{\sin 2b}{2i} \right)^{LT/2} \sum_{\{s_{\tau,j}\}} e^{-i \sum_{\tau=1}^T \sum_{j=1}^L (J s_{\tau,j} s_{\tau,j+1} + J' s_{\tau,j} s_{\tau+1,j} + h s_{\tau,j})}, \end{aligned} \quad (\text{S-1})$$

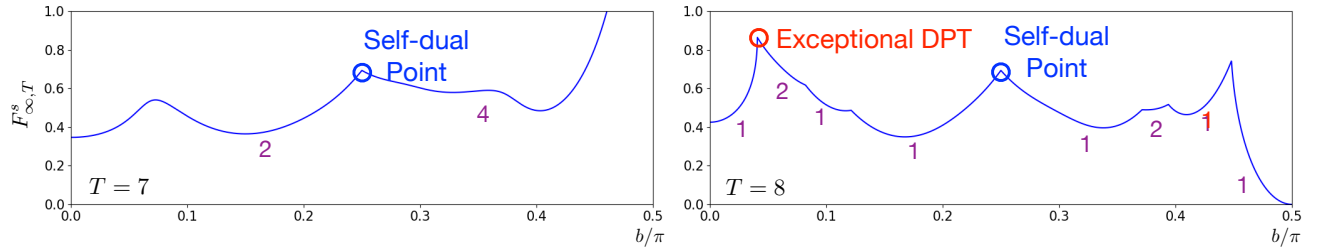


FIG. S-1: (Real part of) dynamical free energy  $F_{\infty,T}^s$  as a function of  $b$  for different transient times  $T$ . As varying  $b$ , the exceptional DPT occurs for  $T = 8$ , which is prohibited for  $T = 7$ . Purple numbers denotes  $n_{\text{deg}}$  for each phase. We use  $h = 0.5$  and  $J = 0.25\pi$ .

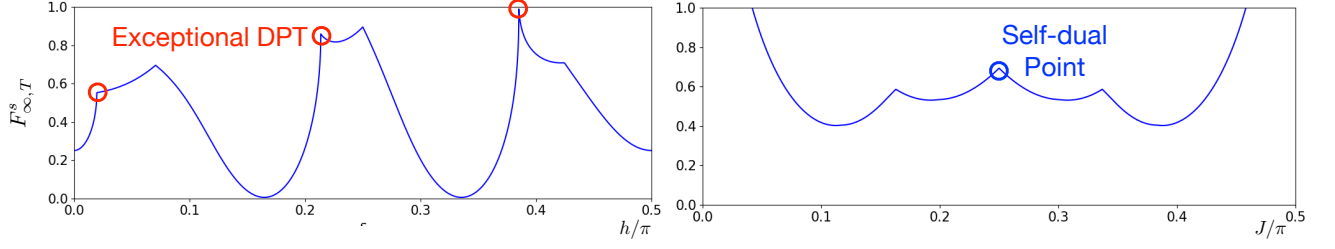


FIG. S-2: (Real part of) dynamical free energy  $F_{\infty,T}^s$  as a function of (left)  $h$  and (right)  $J$ . As a function of  $h$ , we have several exceptional DPTs, where  $J = 0.25\pi$ ,  $b = 0.05\pi$  and  $T = 6$  are used. On the other hand, no exceptional DPT exists as a function of  $J$  because of the absence of the hidden antiunitary symmetry of  $\tilde{U}$  ( $h = 3$ ,  $b = -0.25\pi$  and  $T = 6$  are used).

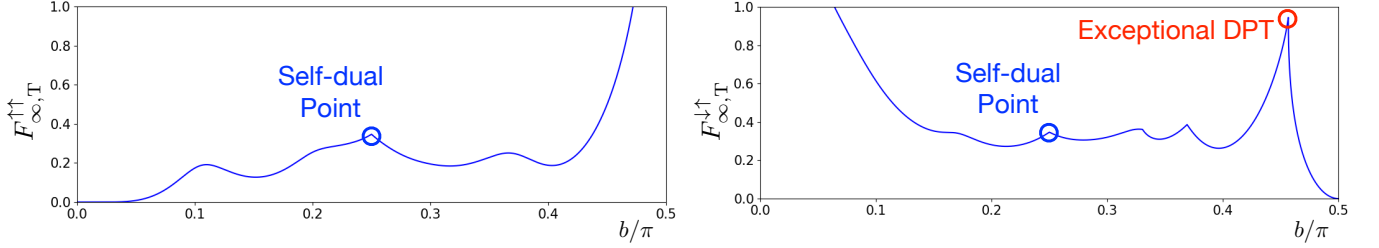


FIG. S-3: (Real part of) dynamical free energy (left)  $F_{\infty,T}^{\uparrow\uparrow}$  and (right)  $F_{\infty,T}^{\downarrow\uparrow}$  as a function of  $b$ . The exceptional DPT occurs only for  $F_{\infty,T}^{\downarrow\uparrow}$ . Note that  $n_{\text{deg}}$  changes from 2 to 1 at the exceptional DPT as increasing  $b$ . We use  $h = 2$ ,  $J = -0.25\pi$  and  $T = 7$  for both of the data.

where  $|\mathbf{s}_\tau\rangle$  are the computational basis,  $s_{\tau,j}$  are classical spin variables taking  $\pm 1$ , and  $J' = -\frac{\pi}{4} - \frac{i}{2} \log \tan b$ . On the other hand, we can consider the dual operator of  $U$ ,

$$\tilde{U}'_s = e^{-i \sum_{\tau=1}^T \tilde{b} \sigma_\tau^x} e^{-i \sum_{\tau=1}^T (\tilde{J} \sigma_\tau^z \sigma_{\tau+1}^z + h \sigma_\tau^z)}. \quad (\text{S-2})$$

We then find

$$\text{Tr}[\tilde{U}'_s{}^L] = \left( \frac{\sin 2\tilde{b}}{2i} \right)^{LT/2} \sum_{\{s_{\tau,j}\}} e^{-i \sum_{\tau=1}^T \sum_{j=1}^L (\tilde{J}' s_{\tau,j} s_{\tau,j+1} + \tilde{J} s_{\tau,j} s_{\tau+1,j} + h s_{\tau,j})} \quad (\text{S-3})$$

with  $\tilde{J}' = -\frac{\pi}{4} - \frac{i}{2} \log \tan \tilde{b}$ . Thus, introducing a normalization constant

$$C = \frac{1}{2} \left( \frac{\sin 2b}{\sin 2\tilde{b}} \right)^{\frac{LT}{2}} \quad (\text{S-4})$$

and setting  $\tilde{b} = \arctan[e^{2i(J+\pi/4)}] = \frac{i}{2} \log \left( \frac{1+e^{2iJ}}{1-e^{2iJ}} \right) = -\frac{\pi}{4} - \frac{i}{2} \log \tan J$  (to satisfy  $\tilde{J}' = J$ ) and  $\tilde{J} = J'$ , we have  $\tilde{U}_s = C \tilde{U}'_s$ ,  $\text{Tr}[U^T]/2^L = \text{Tr}[\tilde{U}^L]$  or

$$F_{L,T}^s = -\frac{\log |\text{Tr}[\tilde{U}_s^L]|}{L}. \quad (\text{S-5})$$

Next,  $\tilde{U}_{\uparrow\uparrow/\downarrow\uparrow}$  can be calculated similarly. We show that they are represented as

$$\tilde{U}_{\uparrow\uparrow/\downarrow\uparrow} = C' e^{-i \sum_{\tau=1}^{T-1} \tilde{b} \sigma_\tau^x} e^{-i \sum_{\tau=1}^{T-2} \tilde{J} \sigma_\tau^z \sigma_{\tau+1}^z - i \sum_{\tau=1}^{T-1} h \sigma_\tau^z - i \tilde{J} (\sigma_1^z + I \sigma_{T-1}^z)} \quad (\text{S-6})$$

with the open boundary condition, where  $C' = (\sin 2b/2i)^{1/2} (\sin 2b/\sin 2\tilde{b})^{(T-1)/2} e^{-i(h+J)}$ , and  $I = 1$  ( $-1$ ) for



$\tilde{U}_{\uparrow\uparrow}(\tilde{U}_{\downarrow\downarrow})$ . To see this, we notice (for  $|\psi_f\rangle = |\uparrow \cdots \uparrow\rangle / |\downarrow \cdots \downarrow\rangle$ )

$$\begin{aligned} \langle \psi_f | U^T | \uparrow \cdots \uparrow \rangle &= \sum_{\{\mathbf{s}_\tau\}} \langle \psi_f | U | \mathbf{s}_{T-1} \rangle \cdots \langle \mathbf{s}_1 | U | \uparrow \cdots \uparrow \rangle \\ &= \left( \frac{\sin 2b}{2i} \right)^{LT/2} \sum_{\{s_{\tau,j}\}} e^{-i \sum_{\tau=1}^{T-1} \sum_{j=1}^L J s_{\tau,j} s_{\tau,j+1} + h s_{\tau,j} - i \sum_{\tau=1}^{T-2} \sum_{j=1}^L J' s_{\tau,j} s_{\tau+1,j} - i \sum_{j=1}^L \{(J+h) + J' s_{1,j} + J' I s_{T-1,j}\}}, \end{aligned} \quad (\text{S-7})$$

where  $I = 1$  for  $|\psi_f\rangle = |\uparrow \cdots \uparrow\rangle$  and  $I = -1$  for  $|\psi_f\rangle = |\downarrow \cdots \downarrow\rangle$ . To construct dual operators, we consider  $(T-1)$ -spins along time with open boundary condition. In fact, if we assume Eq. (S-6), we find

$$F_{L,T}^{\uparrow\uparrow/\downarrow\downarrow} = -\frac{\log |\text{Tr}[\tilde{U}_{\uparrow\uparrow/\downarrow\downarrow}^L]|}{L}. \quad (\text{S-8})$$

### SUPPLEMENTAL NOTE 3: EXISTENCE OF ANTIUNITARY SYMMETRY

Here, we describe in detail the antiunitary (AUS) of the spacetime-dual operator. First, we show that the spacetime-dual operator  $\tilde{U}_s$  with  $J = \frac{\pi}{4} + \frac{n\pi}{2}$  ( $n \in \mathbb{Z}$ ) satisfies

$$V \tilde{U}_s^* V^\dagger = e^{i\phi} \tilde{U}_s, \quad (\text{S-9})$$

where

$$V = \prod_{\tau=1}^T e^{i\frac{\pi}{2}\sigma_\tau^y} \quad (\text{S-10})$$

and  $\phi \in \mathbb{R}$ .

For  $J = \frac{\pi}{4} + \frac{n\pi}{2}$  ( $n \in \mathbb{Z}$ ),  $\tilde{b} = \pm\pi/4$  becomes real. Noticing  $\tilde{J} = -\frac{\pi}{4} - \frac{i}{2} \log \tan b = -\tilde{J}^* - \frac{\pi}{2}$ , the left-hand side of Eq. (S-9) becomes

$$\begin{aligned} V \tilde{U}_s^* V^\dagger &= C V e^{i \sum_{\tau=1}^T \tilde{b} \sigma_\tau^x} V^\dagger V e^{i \sum_{\tau=1}^T (\tilde{J}^* \sigma_\tau^z \sigma_{\tau+1}^z + h \sigma_\tau^z)} V^\dagger \\ &= e^{-i \sum_{\tau=1}^T \tilde{b} \sigma_\tau^x} e^{i \sum_{\tau=1}^T (\tilde{J}^* \sigma_\tau^z \sigma_{\tau+1}^z - h \sigma_\tau^z)} \\ &= e^{-i \sum_{\tau=1}^T \tilde{b} \sigma_\tau^x} e^{-i \sum_{\tau=1}^T (\tilde{J} \sigma_\tau^z \sigma_{\tau+1}^z + h \sigma_\tau^z)} e^{-i \frac{\pi}{2} \sum_{\tau=1}^T \sigma_\tau^z \sigma_{\tau+1}^z} \\ &= \tilde{U}_s \prod_{\tau=1}^T (-i \sigma_\tau^z \sigma_{\tau+1}^z) = (-i)^T \tilde{U}_s, \end{aligned} \quad (\text{S-11})$$

which is the right-hand side. Since  $V V^* = \mathbb{I}$  for even  $T$  and  $-\mathbb{I}$  for odd  $T$ ,  $\tilde{U}_s$  belongs to Class AI for even  $T$  and Class AII for odd  $T$ .

Next, we show that  $\tilde{U}_{\downarrow\uparrow}$  with  $J = \frac{\pi}{4} + \frac{n\pi}{2}$  ( $n \in \mathbb{Z}$ ) satisfies

$$V \tilde{U}_{\downarrow\uparrow}^* V^\dagger = e^{i\phi} \tilde{U}_{\downarrow\uparrow}, \quad (\text{S-12})$$

where

$$V = \mathcal{P} \prod_{\tau=1}^{T-1} e^{i\frac{\pi}{2}\sigma_\tau^y} \quad (\text{S-13})$$

and  $\phi \in \mathbb{R}$ . Here,  $\mathcal{P}$  is the parity operator exchanging the site  $\tau$  and  $T - \tau$ . In fact, the left-hand side of Eq. (S-12) becomes

$$\begin{aligned} V \tilde{U}_{\downarrow\uparrow}^* V^\dagger &= C'^* V e^{i \sum_{\tau=1}^{T-1} \tilde{b} \sigma_\tau^x} V^\dagger V e^{i \sum_{\tau=1}^{T-2} \tilde{J}^* \sigma_\tau^z \sigma_{\tau+1}^z + i \sum_{\tau=1}^{T-1} h \sigma_\tau^z + i \tilde{J}^* (\sigma_1^z - \sigma_{T-1}^z)} V^\dagger \\ &= e^{i\zeta} C' e^{-i \sum_{\tau=1}^{T-1} \tilde{b} \sigma_\tau^x} e^{i \sum_{\tau=1}^{T-2} \tilde{J}^* \sigma_\tau^z \sigma_{\tau+1}^z - i \sum_{\tau=1}^{T-1} h \sigma_\tau^z - i \tilde{J}^* (-\sigma_1^z + \sigma_{T-1}^z)} \\ &= e^{i\zeta} \tilde{U}_{\downarrow\uparrow} e^{-i \frac{\pi}{2} \sum_{\tau=1}^{T-1} \sigma_\tau^z \sigma_{\tau+1}^z + i \frac{\pi}{2} (-\sigma_1^z + \sigma_{T-1}^z)} \\ &= e^{i\zeta} \tilde{U}_{\downarrow\uparrow} \sigma_1^z \sigma_{T-1}^z \prod_{\tau=1}^{T-1} (-i \sigma_\tau^z \sigma_{\tau+1}^z) \\ &= e^{i\zeta} (-i)^{T-1} \tilde{U}_{\downarrow\uparrow}, \end{aligned} \quad (\text{S-14})$$

which is the right-hand side. Here, we have used  $\tilde{b} \in \mathbb{R}$  for  $J = \frac{\pi}{4} + \frac{n\pi}{2}$  ( $n \in \mathbb{Z}$ ),  $\tilde{J}^* = -(\tilde{J} + \pi/2)$ ,  $C'^*/C' = e^{i\zeta}$  ( $\zeta \in \mathbb{R}$ ), and  $\mathcal{P}\sigma_1\mathcal{P} = \sigma_{T-1}$ . Since  $VV^* = \mathbb{I}$  for odd  $T$  and  $-\mathbb{I}$  for even  $T$ ,  $\tilde{U}_{\downarrow\uparrow}$  belongs to Class AI for odd  $T$  and Class AII for even  $T$ .

We note that the minus sign associated with the exchange between  $\sigma_1^z - \sigma_{T-1}^z$  under parity operation is essential for this antiunitary symmetry. This is not possible for  $\tilde{U}_{\uparrow\uparrow}$ , where  $\sigma_1^z + \sigma_{T-1}^z$  is invariant under parity operation.

#### SUPPLEMENTAL NOTE 4: GENERALIZED CORRELATION FUNCTION AND ITS BEHAVIOR IN SMALL SYSTEMS

In the main text, we have defined the generalized correlation function

$$C(r) = \langle \sigma_1 \sigma_{r+1} \rangle_{\text{gexp}} - \langle \sigma_1 \rangle_{\text{gexp}} \langle \sigma_{r+1} \rangle_{\text{gexp}}, \quad (\text{S-15})$$

where

$$\langle A \rangle_{\text{gexp}} = \frac{\text{Tr}[AU^T]}{\text{Tr}[U^T]}. \quad (\text{S-16})$$

To calculate this generalized correlation function, we first note the dual representation

$$C(r) = \left| \frac{\text{Tr}[\tilde{U}^{L-r} \sigma^z \tilde{U}^r \sigma^z]}{\text{Tr}[\tilde{U}^L]} - \left( \frac{\text{Tr}[\tilde{U}^L \sigma^z]}{\text{Tr}[\tilde{U}^L]} \right)^2 \right|, \quad (\text{S-17})$$

where we have used the fact that  $\sigma^z$  is invariant under dual transformation (see Supplemental Note 2). Inserting the eigenstate decomposition of  $\tilde{U} = \sum_{\alpha} \lambda_{\alpha} |\phi_{\alpha}\rangle \langle \chi_{\alpha}|$ , we have

$$C(r) \rightarrow \left| \left( \frac{\lambda_1}{\lambda_0} \right)^r \langle \chi_0 | \sigma^z | \phi_1 \rangle \langle \chi_1 | \sigma^z | \phi_0 \rangle \right| \quad (\text{S-18})$$

for  $b \lesssim b_c$  and large  $L$ . Here, 0 and 1 respectively indicate the labels of eigenvalues with the largest and the second largest modulus. From this the generalized correlation length is obtained as  $\xi_{\text{cor}} = -(\ln \lambda_1/\lambda_0)^{-1} \simeq \lambda_0/(\lambda_0 - \lambda_1)$  and behaves as  $\sim (b_c - b)^{-1/2}$  near the exceptional DPT.

For  $b > b_c$ ,  $C(r)$  contains a term  $e^{-ir\Delta}$  even in the thermodynamic limit, where  $\Delta$  ( $< \pi$ ) is the difference between angles of two complex-conjugate eigenvalues. Thus the oscillation length becomes  $\xi_{\text{osc}} = \frac{2\pi}{\Delta}$  and behaves as  $\sim (b - b_c)^{-1/2}$  near the exceptional DPT.

While the true DPT occurs in the thermodynamic limit, qualitative signature of AUS-unbroken and AUS-broken phases are already captured even for finite system sizes with the generalized correlation function. In Fig. S-4, we show the (normalized) generalized correlation function for different system size  $L$ . Even for  $L = 10$ , which has been prepared in experiments of trapped ions [4], we find clear difference between AUS-unbroken ( $b < b_c \simeq 0.0257\pi$ ) and AUS-broken ( $b > b_c$ ) regime. Indeed,  $C(r)$  decays fast for the former but does not decay for the latter. If we consider  $L = 20$ , we can also see the oscillatory behavior in the AUS-broken regime: note that the oscillation length is evaluated as  $\xi_{\text{osc}} \simeq 10.4$  for  $b = 0.03\pi$  and  $\xi_{\text{osc}} \simeq 8.5$  for  $b = 0.0325\pi$ .

#### SUPPLEMENTAL NOTE 5: OTHER MODELS THAT EXHIBIT EXCEPTIONAL DPT

##### Floquet unitary circuits

Here, we describe in detail that exceptional DPT can occur in certain Floquet unitary circuits, in addition to our stroboscopic Ising model. We assume that the system size  $L$  is even and consider the unitary circuit given in the form as

$$U = \prod_{j:\text{even}} \mathcal{U}_{j,j+1} \prod_{j:\text{odd}} \mathcal{U}_{j,j+1}, \quad (\text{S-19})$$

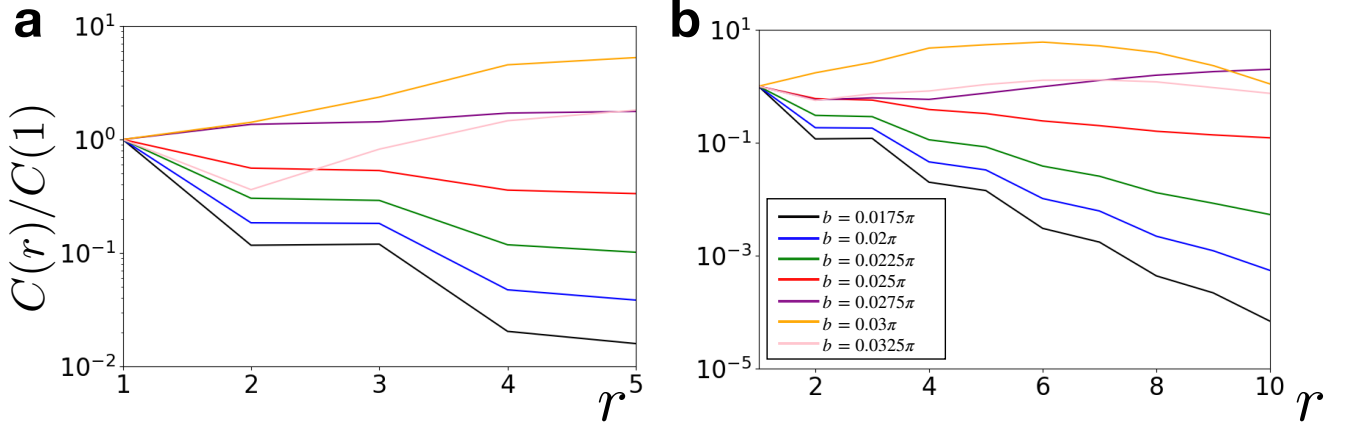


FIG. S-4: Normalized generalized correlation function  $C(r)/C(0)$  for different values of  $b$ . (a) Results for  $L = 10$ . Clear difference between AUS-unbroken ( $b < b_c \simeq 0.0257\pi$ ) and AUS-broken ( $b > b_c$ ) regime already appears. Indeed,  $C(r)$  decays fast for the former but does not decay for the latter. (b) Results for  $L = 20$ . The oscillatory behavior in the AUS-broken regime arises, where the oscillation length is evaluated as  $\xi_{\text{osc}} \simeq 10.4$  for  $b = 0.03\pi$  and  $\xi_{\text{osc}} \simeq 8.5$  for  $b = 0.0325\pi$ .

which is composed of two-site unitary circuit  $\mathcal{U}_{j,j+1}$  (Fig. S-5). When the dimension of the local Hilbert space is two (i.e., spin-1/2 systems), such two-site unitary circuits can be generally represented as [5]

$$\mathcal{U}_{j,j+1} = e^{i\xi}(u_j \otimes u_{j+1})\mathcal{V}(v_j \otimes v_{j+1}), \quad (\text{S-20})$$

where  $u_j$  and  $v_j$  are one-site unitary operators and  $\xi \in \mathbb{R}$ , and

$$\mathcal{V} = e^{-i(J_1\sigma_j^x\sigma_{j+1}^x + J_2\sigma_j^y\sigma_{j+1}^y + J_3\sigma_j^z\sigma_{j+1}^z)}. \quad (\text{S-21})$$

For simplicity, we assume that  $u_j = u$  and  $v_j = v$  are  $j$ -independent in the following.

We now focus on time evolution for  $T/2$  steps, which correspond to the total time  $T (\in 2\mathbb{N})$ , and the following (real part of) dynamical free energy:

$$F_{L,T/2}^s = -\frac{1}{L} \log |\text{Tr}[U^{T/2}]| + \log 2. \quad (\text{S-22})$$

We require that the spacetime-dual operator  $\tilde{U}$  of  $U$  should satisfy

$$F_{L,T/2}^s = -\frac{1}{L} \log |\text{Tr}[\tilde{U}^{L/2}]|, \quad (\text{S-23})$$

with which  $F_{\infty,T/2}^s$  is given by  $-(\log |\lambda_M|)/2$ .

By considering the dual operators for  $\mathcal{U}_{j,j+1}$  [5], we find

$$\tilde{U} = \frac{1}{4} \prod_{\tau:\text{even}} \tilde{\mathcal{U}}_{\tau,\tau+1} \prod_{\tau:\text{odd}} \tilde{\mathcal{U}}_{\tau,\tau+1}, \quad (\text{S-24})$$

where

$$\tilde{\mathcal{U}}_{\tau,\tau+1} = e^{i\xi}(v^T \otimes u)\tilde{\mathcal{V}}_{\tau,\tau+1}(v \otimes u^T). \quad (\text{S-25})$$

Here,

$$\tilde{\mathcal{V}}_{\tau,\tau+1} = \frac{1}{2}e^{-iJ_3+iJ_-}\sigma_\tau^z\sigma_{\tau+1}^z + \frac{1}{2}e^{-iJ_3-iJ_-} + \frac{1}{2}e^{iJ_3-iJ_+}\sigma_\tau^x\sigma_{\tau+1}^x - \frac{1}{2}e^{iJ_3+iJ_+}\sigma_\tau^y\sigma_{\tau+1}^y \quad (\text{S-26})$$

with  $J_\pm = J_1 \pm J_2$  and  $T$  denotes transposition. It can also be written as [5]

$$\begin{bmatrix} e^{-iJ_3} \cos(J_-) & 0 & 0 & e^{iJ_3} \cos(J_+) \\ 0 & -ie^{-iJ_3} \sin(J_-) & -ie^{iJ_3} \sin(J_+) & 0 \\ 0 & -ie^{iJ_3} \sin(J_+) & -ie^{-iJ_3} \sin(J_-) & 0 \\ e^{iJ_3} \cos(J_+) & 0 & 0 & e^{-iJ_3} \cos(J_-) \end{bmatrix}. \quad (\text{S-27})$$

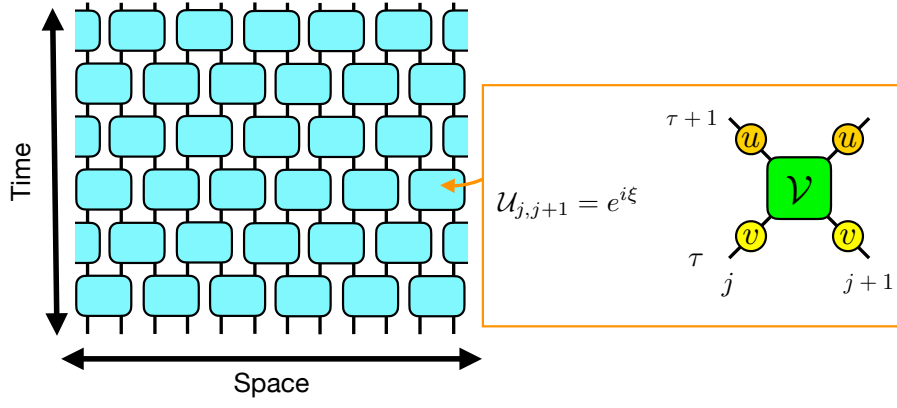


FIG. S-5: Schematic illustration of the Floquet circuit dynamics in Eq. (S-19). We show the example for  $L = 12$  and  $T = 6$ . Each of the block  $\mathcal{U}_{j,j+1}$  can be written as in Eq. (S-20).

### Antiunitary symmetry

To discuss existence of exceptional DPT, we restrict ourselves to  $\xi = 0$  and

$$u = v = e^{-i\frac{\hbar}{2}\sigma^z}. \quad (\text{S-28})$$

To simplify the notation, we consider the unitary transformation for  $\tilde{U} \rightarrow (u \otimes u)\tilde{U}(u^\dagger \otimes u^\dagger)$ , which does not change its eigenvalues, and discuss

$$\tilde{U} = \frac{1}{4} \prod_{\tau:\text{even}} e^{-ih\sigma_\tau^z} e^{-ih\sigma_{\tau+1}^z} \tilde{\mathcal{V}}_{\tau,\tau+1} \prod_{\tau:\text{odd}} e^{-ih\sigma_\tau^z} e^{-ih\sigma_{\tau+1}^z} \tilde{\mathcal{V}}_{\tau,\tau+1} \quad (\text{S-29})$$

In the following, we show that  $\tilde{U}$  has AUS and that the exceptional DPT can exist for nontrivial points  $J_3 = \pi/4$  and  $J_3 = \pi/2$ .

Let us first consider the case for  $J_3 = \pi/2$ . In this case, we show that

$$V = \prod_{\tau=1}^T e^{i\frac{\pi}{2}\sigma_\tau^x} = i^T \prod_{\tau=1}^T \sigma_\tau^x \quad (\text{S-30})$$

becomes AUS. To see this, we note that

$$V\tilde{U}V^\dagger = \frac{1}{4} \prod_{\tau:\text{even}} V_2 e^{-ih(\sigma_\tau^z + \sigma_{\tau+1}^z)} \tilde{\mathcal{V}}_{\tau,\tau+1} V_2^\dagger \prod_{\tau:\text{odd}} V_2 e^{-ih(\sigma_\tau^z + \sigma_{\tau+1}^z)} \tilde{\mathcal{V}}_{\tau,\tau+1} V_2^\dagger, \quad (\text{S-31})$$

where  $V_2$  is a shorthand notation for  $\sigma_\tau^x \sigma_{\tau+1}^x$ . First, nonzero matrix elements of local gates satisfy

$$\begin{aligned} \langle \uparrow\downarrow | V_2 e^{-ih(\sigma_\tau^z + \sigma_{\tau+1}^z)} \tilde{\mathcal{V}}_{\tau,\tau+1} V_2^\dagger | \uparrow\downarrow \rangle &= \langle \uparrow\downarrow | e^{-ih(\sigma_\tau^z + \sigma_{\tau+1}^z)} \tilde{\mathcal{V}}_{\tau,\tau+1} | \uparrow\downarrow \rangle \\ &= \langle \uparrow\downarrow | e^{-ih(\sigma_\tau^z + \sigma_{\tau+1}^z)} \tilde{\mathcal{V}}_{\tau,\tau+1} | \uparrow\downarrow \rangle^* = -\sin J_- \end{aligned} \quad (\text{S-32})$$

$$\begin{aligned} \langle \downarrow\uparrow | V_2 e^{-ih(\sigma_\tau^z + \sigma_{\tau+1}^z)} \tilde{\mathcal{V}}_{\tau,\tau+1} V_2^\dagger | \uparrow\downarrow \rangle &= \langle \uparrow\downarrow | e^{-ih(\sigma_\tau^z + \sigma_{\tau+1}^z)} \tilde{\mathcal{V}}_{\tau,\tau+1} | \downarrow\uparrow \rangle \\ &= \langle \downarrow\uparrow | e^{-ih(\sigma_\tau^z + \sigma_{\tau+1}^z)} \tilde{\mathcal{V}}_{\tau,\tau+1} | \uparrow\downarrow \rangle^* = \sin J_+ \end{aligned} \quad (\text{S-33})$$

$$\begin{aligned} \langle \downarrow\downarrow | V_2 e^{-ih(\sigma_\tau^z + \sigma_{\tau+1}^z)} \tilde{\mathcal{V}}_{\tau,\tau+1} V_2^\dagger | \uparrow\uparrow \rangle &= \langle \uparrow\uparrow | e^{-ih(\sigma_\tau^z + \sigma_{\tau+1}^z)} \tilde{\mathcal{V}}_{\tau,\tau+1} | \downarrow\downarrow \rangle \\ &= -\langle \downarrow\downarrow | e^{-ih(\sigma_\tau^z + \sigma_{\tau+1}^z)} \tilde{\mathcal{V}}_{\tau,\tau+1} | \uparrow\uparrow \rangle^* = i \cos J_+ \end{aligned} \quad (\text{S-34})$$

$$\begin{aligned} \langle \downarrow\downarrow | V_2 e^{-ih(\sigma_\tau^z + \sigma_{\tau+1}^z)} \tilde{\mathcal{V}}_{\tau,\tau+1} V_2^\dagger | \downarrow\downarrow \rangle &= \langle \uparrow\uparrow | e^{-ih(\sigma_\tau^z + \sigma_{\tau+1}^z)} \tilde{\mathcal{V}}_{\tau,\tau+1} | \uparrow\uparrow \rangle \\ &= -\langle \downarrow\downarrow | e^{-ih(\sigma_\tau^z + \sigma_{\tau+1}^z)} \tilde{\mathcal{V}}_{\tau,\tau+1} | \downarrow\downarrow \rangle^* = -ie^{-2ih} \cos J_- \end{aligned} \quad (\text{S-35})$$

$$\begin{aligned} \langle \uparrow\uparrow | V_2 e^{-ih(\sigma_\tau^z + \sigma_{\tau+1}^z)} \tilde{\mathcal{V}}_{\tau,\tau+1} V_2^\dagger | \uparrow\uparrow \rangle &= \langle \downarrow\downarrow | e^{-ih(\sigma_\tau^z + \sigma_{\tau+1}^z)} \tilde{\mathcal{V}}_{\tau,\tau+1} | \downarrow\downarrow \rangle \\ &= -\langle \uparrow\uparrow | e^{-ih(\sigma_\tau^z + \sigma_{\tau+1}^z)} \tilde{\mathcal{V}}_{\tau,\tau+1} | \uparrow\uparrow \rangle^* = -ie^{2ih} \cos J_- \end{aligned} \quad (\text{S-36})$$

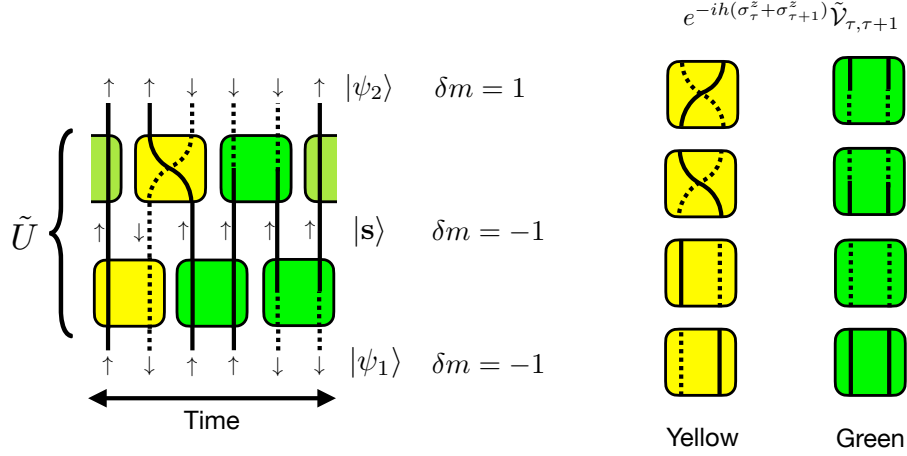


FIG. S-6: Example of a path of computational basis that constitutes a matrix element  $\langle \psi_2 | \tilde{U} | \psi_1 \rangle$  of the spacetime-dual operator  $\tilde{U}$ . We here consider  $|\psi_1\rangle = |\uparrow\downarrow\uparrow\uparrow\downarrow\rangle$  and  $|\psi_2\rangle = |\uparrow\uparrow\downarrow\downarrow\uparrow\rangle$ , and insert a middle state  $|\mathbf{s}\rangle = |\uparrow\downarrow\uparrow\uparrow\uparrow\rangle$ , where black lines denote  $|\uparrow\rangle$  and dotted lines denote  $|\downarrow\rangle$ . These states are transformed by local two-site gates  $e^{-ih(\sigma_\tau^z + \sigma_{\tau+1}^z)} \tilde{\mathcal{V}}_{\tau,\tau+1}$ , which are colored with yellow or green depending on the transformed spin states. By considering difference of magnetization  $\delta m$  between even and odd sites, we can show that green and yellow gates must appear even times.

and other matrix elements are zero, where we have used Eq. (S-27) with  $J_3 = \pi/2$ . From this, while matrix elements of the two-site transitions for  $\{|\uparrow\downarrow\rangle \rightarrow |\uparrow\downarrow\rangle, |\uparrow\downarrow\rangle \rightarrow |\downarrow\uparrow\rangle, |\downarrow\uparrow\rangle \rightarrow |\downarrow\uparrow\rangle, |\downarrow\uparrow\rangle \rightarrow |\uparrow\downarrow\rangle\}$  (yellow gates in Fig. S-6) are invariant under complex conjugation, those of the two-site transitions for  $\{|\uparrow\uparrow\rangle \rightarrow |\uparrow\uparrow\rangle, |\uparrow\uparrow\rangle \rightarrow |\downarrow\downarrow\rangle, |\downarrow\downarrow\rangle \rightarrow |\uparrow\uparrow\rangle, |\downarrow\downarrow\rangle \rightarrow |\downarrow\downarrow\rangle\}$  (green gates in Fig. S-6) acquire a minus sign under complex conjugation.

Now, consider matrix elements of  $\tilde{U}$  as a sum of the paths of the computational states. For example, we can consider a matrix element

$$\langle \uparrow\uparrow\downarrow\downarrow\uparrow | \tilde{U} | \uparrow\downarrow\uparrow\uparrow\downarrow \rangle = \frac{1}{4} \sum_{\mathbf{s}} \langle \uparrow\uparrow\downarrow\downarrow\uparrow | \prod_{\tau:\text{even}} e^{-ih(\sigma_\tau^z + \sigma_{\tau+1}^z)} \tilde{\mathcal{V}}_{\tau,\tau+1} |\mathbf{s}\rangle \langle \mathbf{s}| \prod_{\tau:\text{odd}} e^{-ih(\sigma_\tau^z + \sigma_{\tau+1}^z)} \tilde{\mathcal{V}}_{\tau,\tau+1} | \uparrow\downarrow\uparrow\uparrow\downarrow \rangle \quad (\text{S-37})$$

for  $T = 6$ . In Fig. S-6, we show one of the paths that corresponds to  $|\mathbf{s}\rangle = |\uparrow\downarrow\uparrow\uparrow\uparrow\rangle$  for this example. Then, generally, we can show that each of the paths must include even times of two-site transitions for green gates, and even times for yellow gates. To see this, we focus on the difference  $\delta m$  between even and odd sites (in the time direction). For the above example,  $\delta m$  is  $-1$  for  $|\uparrow\downarrow\uparrow\uparrow\downarrow\rangle$  and  $|\uparrow\downarrow\uparrow\uparrow\uparrow\rangle$ , and  $+1$  for  $|\uparrow\uparrow\downarrow\downarrow\uparrow\rangle$ , where we assign  $-\frac{1}{2}$  for  $|\downarrow\rangle$  and  $\frac{1}{2}$  for  $|\uparrow\rangle$ . When we consider a general matrix element  $\langle \psi_2 | \tilde{U} | \psi_1 \rangle \propto \sum_{\mathbf{s}} \langle \psi_2 | \cdots | \mathbf{s} \rangle \langle \mathbf{s} | \cdots | \psi_1 \rangle$ ,  $\delta m$  for  $|\psi_1\rangle, |\psi_2\rangle, |\mathbf{s}\rangle$  have the same even-odd parity. It is also clear that there are odd/even numbers of yellow gates for odd/even  $\delta m$  in the first half of the path ( $\langle \mathbf{s} | \cdots | \psi_1 \rangle$ ) and for odd/even  $-\delta m$  in the second half of the path ( $\langle \psi_2 | \cdots | \mathbf{s} \rangle$ ). Since  $\delta m$  and  $-\delta m$  have the same even-odd parity, the total number of the yellow gates in the path is even. Because the total number of all gates is even, the number of green gates is also even.

Owing to the even-time appearance of the green gates, the  $-1$  phase under complex conjugation for the green gates cancels out for every path. Then we finally have

$$\langle \psi_2 | V \tilde{U} V^\dagger | \psi_1 \rangle = \langle \psi_2 | \tilde{U} | \psi_1 \rangle^* \quad (\text{S-38})$$

for every matrix element, i.e.,  $\tilde{U}$  has AUS. We note that, since  $V^2 = 1$  for all  $T$ ,  $\tilde{U}$  belongs to symmetry class AI and can have an exceptional point irrespective of  $T$ , in contrast with the case for the stroboscopic Ising model.

The symmetry structure for  $J_3 = \pi/4$  can be discussed similarly: we find that

$$V = \prod_{\tau:\text{odd}} e^{i\frac{\pi}{2}\sigma_\tau^x} \prod_{\tau:\text{even}} e^{i\frac{\pi}{2}\sigma_\tau^y} = i^T \prod_{\tau:\text{odd}} \sigma_\tau^x \prod_{\tau:\text{even}} \sigma_\tau^y \quad (\text{S-39})$$

becomes AUS in this case. To see this, we note that

$$V \tilde{U} V^\dagger = \frac{1}{4} \prod_{\tau:\text{even}} V_2' e^{-ih(\sigma_\tau^z + \sigma_{\tau+1}^z)} \tilde{\mathcal{V}}_{\tau,\tau+1} V_2'^\dagger \prod_{\tau:\text{odd}} V_2 e^{-ih(\sigma_\tau^z + \sigma_{\tau+1}^z)} \tilde{\mathcal{V}}_{\tau,\tau+1} V_2^\dagger, \quad (\text{S-40})$$

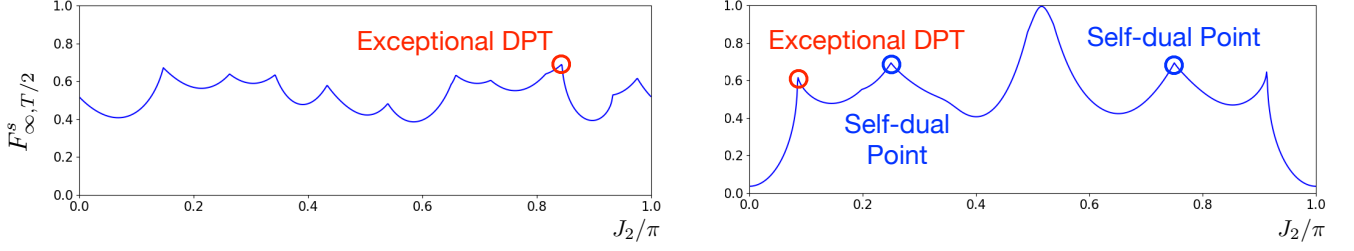


FIG. S-7: (Real part of) dynamical free energy  $F_{\infty, T/2}^s$  as a function of  $J_2$ . We choose parameters as (left)  $J_3 = \pi/2, J_1 = 0.15\pi, h = 1.0, T = 6$  and (right)  $J_3 = \pi/4, J_1 = 0.47\pi, h = 1.0, T = 8$ . As varying  $J_2$ , the exceptional DPT occurs for both of the cases, as well as DPTs through self-dual points for  $J_3 = \pi/4$ .

where  $V_2$  and  $V_2'$  are shorthand notations for  $\sigma_\tau^x \sigma_{\tau+1}^y$  and  $\sigma_\tau^y \sigma_{\tau+1}^x$ , respectively. Again, we can calculate nonzero matrix elements of local gates as

$$\begin{aligned} \langle \uparrow \downarrow | V_2 e^{-ih(\sigma_\tau^z + \sigma_{\tau+1}^z)} \tilde{V}_{\tau, \tau+1} V_2^\dagger | \uparrow \downarrow \rangle &= \langle \uparrow \downarrow | e^{-ih(\sigma_\tau^z + \sigma_{\tau+1}^z)} \tilde{V}_{\tau, \tau+1} | \uparrow \downarrow \rangle \\ &= i \langle \uparrow \downarrow | e^{-ih(\sigma_\tau^z + \sigma_{\tau+1}^z)} \tilde{V}_{\tau, \tau+1} | \uparrow \downarrow \rangle^* = -ie^{-\frac{\pi}{4}i} \sin J_- \end{aligned} \quad (\text{S-41})$$

$$\begin{aligned} \langle \uparrow \uparrow | V_2 e^{-ih(\sigma_\tau^z + \sigma_{\tau+1}^z)} \tilde{V}_{\tau, \tau+1} V_2^\dagger | \uparrow \uparrow \rangle &= -\langle \uparrow \downarrow | e^{-ih(\sigma_\tau^z + \sigma_{\tau+1}^z)} \tilde{V}_{\tau, \tau+1} | \downarrow \uparrow \rangle \\ &= i \langle \downarrow \uparrow | e^{-ih(\sigma_\tau^z + \sigma_{\tau+1}^z)} \tilde{V}_{\tau, \tau+1} | \uparrow \downarrow \rangle^* = -e^{-\frac{\pi}{4}i} \sin J_+ \end{aligned} \quad (\text{S-42})$$

$$\begin{aligned} \langle \downarrow \downarrow | V_2 e^{-ih(\sigma_\tau^z + \sigma_{\tau+1}^z)} \tilde{V}_{\tau, \tau+1} V_2^\dagger | \uparrow \uparrow \rangle &= -\langle \uparrow \uparrow | e^{-ih(\sigma_\tau^z + \sigma_{\tau+1}^z)} \tilde{V}_{\tau, \tau+1} | \downarrow \downarrow \rangle \\ &= -i \langle \downarrow \downarrow | e^{-ih(\sigma_\tau^z + \sigma_{\tau+1}^z)} \tilde{V}_{\tau, \tau+1} | \uparrow \uparrow \rangle^* = -ie^{-\frac{\pi}{4}i} \cos J_+ \end{aligned} \quad (\text{S-43})$$

$$\begin{aligned} \langle \downarrow \downarrow | V_2 e^{-ih(\sigma_\tau^z + \sigma_{\tau+1}^z)} \tilde{V}_{\tau, \tau+1} V_2^\dagger | \downarrow \downarrow \rangle &= \langle \uparrow \uparrow | e^{-ih(\sigma_\tau^z + \sigma_{\tau+1}^z)} \tilde{V}_{\tau, \tau+1} | \uparrow \uparrow \rangle \\ &= -i \langle \downarrow \downarrow | e^{-ih(\sigma_\tau^z + \sigma_{\tau+1}^z)} \tilde{V}_{\tau, \tau+1} | \downarrow \downarrow \rangle^* = e^{-\frac{\pi}{4}i} e^{-2ih} \cos J_- \end{aligned} \quad (\text{S-44})$$

$$\begin{aligned} \langle \uparrow \uparrow | V_2 e^{-ih(\sigma_\tau^z + \sigma_{\tau+1}^z)} \tilde{V}_{\tau, \tau+1} V_2^\dagger | \uparrow \uparrow \rangle &= \langle \downarrow \downarrow | e^{-ih(\sigma_\tau^z + \sigma_{\tau+1}^z)} \tilde{V}_{\tau, \tau+1} | \downarrow \downarrow \rangle \\ &= -i \langle \uparrow \uparrow | e^{-ih(\sigma_\tau^z + \sigma_{\tau+1}^z)} \tilde{V}_{\tau, \tau+1} | \uparrow \uparrow \rangle^* = e^{-\frac{\pi}{4}i} e^{2ih} \cos J_-, \end{aligned} \quad (\text{S-45})$$

where  $J_3 = \pi/4$  is used. Again, since the two-site transitions for  $\{|\uparrow\uparrow\rangle \rightarrow |\uparrow\uparrow\rangle, |\uparrow\uparrow\rangle \rightarrow |\downarrow\downarrow\rangle, |\downarrow\downarrow\rangle \rightarrow |\uparrow\uparrow\rangle, |\downarrow\downarrow\rangle \rightarrow |\downarrow\downarrow\rangle\}$  appear even times. Consequently, complex conjugation leaves the overall factor  $i^T$ , i.e.,

$$\langle \psi_2 | V \tilde{U} V^\dagger | \psi_1 \rangle = (-1)^{T/2} \langle \psi_2 | \tilde{U} | \psi_1 \rangle^*, \quad (\text{S-46})$$

meaning that  $\tilde{U}$  has AUS. We note that  $VV^* = (-1)^{T/2}$  and thus  $\tilde{U}$  belongs to Class AI/AII for even/odd  $T/2$ . Thus, the exceptional DPT occurs only when  $T/2$  is even for  $J_3 = \pi/4$ .

### Dynamical phase transitions

We demonstrate that the exceptional DPT occurs for the above Floquet circuit model. In Fig. S-7, we show dynamical free energy  $F_{\infty, T/2}^s$  for  $J_3 = \pi/2$  and  $J_3 = \pi/4$ , where we vary  $J_2$ . We find that the exceptional DPTs occur for both of the cases, thanks to the antiunitary symmetry hidden in the spacetime-dual operator  $\tilde{U}$ . We also note that, there appear DPTs through the self-dual points [5] with  $J_3 = \pi/4$  and  $J_2 = \pi/4, 3\pi/4$ , where  $F_{\infty, T/2}^s$  universally takes  $\log 2$ .

- 
- [1] Akila, M., Waltner, D., Gutkin, B. & Guhr, T. Particle-time duality in the kicked ising spin chain. *Journal of Physics A: Mathematical and Theoretical* **49**, 375101 (2016).  
[2] Bertini, B., Kos, P. & Prosen, T. Exact spectral form factor in a minimal model of many-body quantum chaos. *Phys. Rev. Lett.* **121**, 264101 (2018). URL <https://link.aps.org/doi/10.1103/PhysRevLett.121.264101>.



- [3] Bertini, B., Kos, P. & Prosen, T. Entanglement spreading in a minimal model of maximal many-body quantum chaos. *Phys. Rev. X* **9**, 021033 (2019). URL <https://link.aps.org/doi/10.1103/PhysRevX.9.021033>.
- [4] Zhang, J. *et al.* Observation of a discrete time crystal. *Nature* **543**, 217 (2017).
- [5] Bertini, B., Kos, P. & Prosen, T. c. v. Exact correlation functions for dual-unitary lattice models in  $1+1$  dimensions. *Phys. Rev. Lett.* **123**, 210601 (2019). URL <https://link.aps.org/doi/10.1103/PhysRevLett.123.210601>.